Visco-acoustic Wave-equation Traveltime Inversion with Correct and Incorrect Attenuation Profiles

*Han Yu[*1,2], Yuqing Chen[*1], Bowen Guo[1], Gerard T. Schuster[1]*
1. Division of Physical Sciences and Engineering, King Abdullah University of Science and Technology, Thuwal 23955-6900, Saudi Arabia; 2. Jiangsu Key Lab of Big Data Security and Intelligent Processing, School of Computer Science, Nanjing University of Posts and Telecommunications, Nanjing 210003, China.

SUMMARY

A visco-acoustic wave-equation traveltime inversion method is presented that inverts for a shallow subsurface velocity distribution with correct and incorrect attenuation profiles. Similar to the classical wave equation traveltime inversion, this method applies the misfit functional that minimizes the first break differences between the observed and predicted data. Although, WT can partly avoid the cycle skipping problem, an initial velocity model approaches to the right or wrong velocity models under different setups of the attenuation profiles. However, with a *Q* model far away from the real model, the inverted tomogram is obviously different from the true velocity model while a small change of the *Q* model does not improve the inversion quality in a strong manner if low frequency information is not lost. .

INTRODUCTION

Conventional full waveform inversion (FWI) is expected to invert for a highly resolved subsurface velocity distribution that minmizes the waveform residuals between the predicted and the observed traces (Tarantola, 2005; Virieux and Operto, 2009). However, this misfit functional is easily trapped into a local minimum due to its high non-linearlity with respect to the velocity variation. Therefore, wave-equation traveltime inversion (WT) (Luo and Schuster, 1991a,b) was proposed to quasi-linearly invert for the low-intermediate wavenumber parts of the background velocity model. As a skeletonized version of the traveltime differences, it largely mitigates the cycle skipping problem and presents a better convergence property than the traditionial FWI. WT can iteratively approach to a convincing starting model for full waveform inversion, or jointly and gradually invert for the detailed subsurface structures with FWI (Feng and Schuster, 2016). However, strong subsurface attenuation leads to the distortion of amplitudes and phases of the first arrivals and it should not be neglected when migrating or inverting the near-surface data (Aki and Ricahrds, 2002). Otherwise, the defocusing or mis-positioning of reflectors in the deeper part cannot be avoided (Dutta and Schuster, 2014). It is thus necessary to take the attenuation factor into account when using WT on near-surface data. .

In this paper, we extend the WT method by taking into account the attentuation using a system of visco-acoustic wave equations. The gradients are computed by smearing the traveltime residuals along the wavepaths with correct and incorrect input of *Q*. A sensitivity test of WT under different *Q* models is also presented. .

THEORY AND METHODOLOGY

Using the traveltime misfit function,

$$\varepsilon = \tfrac{1}{2}\sum_{s,g}\left(\Delta\tau^t(\mathbf{g},\mathbf{s})\right)^2, \tag{1}$$

where $\Delta\tau^t(\mathbf{g},\mathbf{s}) = \tau_{obs}(\mathbf{g},\mathbf{s}) - \tau_{cal}(\mathbf{g},\mathbf{s})$ represents the traveltime residual between the observed and the calculated data from a source **s** to a receiver **g**. WT can be extended to invert for the velocity distribution based on the visco-acoustic wave equation. The velocity model $c(\mathbf{x})$ can be iteratively updated by any gradient or non-gradient based methods as

$$c(\mathbf{x})_{n+1} = c(\mathbf{x})_n + \alpha_n\beta(\mathbf{x})_n, \tag{2}$$

where α, β and n are respectively the step length, the search direction and the iteration index. The Fréchet derivative $\partial\Delta\tau^t/\partial c$ can be obtained by the implicit function theorem as

$$\frac{\partial\Delta\tau^t}{\partial c} = -\frac{\partial\dot{F}/\partial c}{\partial\dot{F}/\partial\Delta\tau^t}, \tag{3}$$

where $\dot{F}$ is the time derivative of a crosscorrelation equation between the predicted $p(\mathbf{g},t+\Delta\tau^t|\mathbf{s},0)$ and the observed data $p(\mathbf{g},t|\mathbf{s},0)^{obs}$,

$$\dot{F}\left(\mathbf{s},\mathbf{g},\Delta\tau^t\right) = \int_0^T p\left(\mathbf{g},t\,|\,\mathbf{s},0\right)^{obs}\,\dot{p}\left(\mathbf{g},t+\Delta\tau^t\,|\,\mathbf{s},0\right)dt = 0\,. \tag{4}$$

The visco-acoustic wave equation, which we assume the wave propagation honors (Blanch et al., 1995) for a given velocity *c* and *Q* model in the spatial-temporal domain, is used to compute the pressure seismogram by

$$\begin{aligned}
&\frac{\partial P}{\partial t} + \kappa(\tau+1)(\nabla\cdot\mathbf{v}) + r_p = S(\mathbf{x}_s,t),\\
&\frac{\partial\mathbf{v}}{\partial t} + \frac{1}{\rho}\nabla P = 0,\\
&\frac{\partial r_p}{\partial t} + \frac{1}{\tau_\sigma}\left(r_p + \tau\kappa(\nabla\cdot\mathbf{v})\right) = 0,
\end{aligned} \tag{5}$$

where $\mathbf{v} = \{v_x, v_y, v_z\}$ is the particle velocity vector, P represents pressure, r_p indicates the memory variable, $\kappa = \rho c^2$, a product of the density ρ and the square of velocity term c, represents the bulk modulus of the medium and $S(\mathbf{x}_s,t)$ represents a bandlimited source term at $\mathbf{x} = \mathbf{x}_s$ and time t. The parameter τ is related to the stress and strain relaxation parameters τ_σ and τ_ε, and the quality factor Q by,

$$\begin{aligned} \tau_\sigma &= \left(\sqrt{1+Q^2} - 1/Q\right)/\omega, \\ \tau_\varepsilon &= \left(\sqrt{1+Q^2} + 1/Q\right)/\omega, \\ \tau &= \tau_\varepsilon/\tau_\sigma . \end{aligned} \tag{6}$$

Here, ω is the selected reference angular frequency and is usually chosen to be the centroid frequency of the source wavelet (Robertson et al., 1994).

Combining equations (2) and (3) yields the traveltime misfit gradients for the velocity parameter c:

$$\beta = \frac{1}{c^3(\mathbf{x})}\sum_{s,g}\int_0^T dt\left[\dot{g}_{bk}(\mathbf{x},t\,|\,\mathbf{g},0) * \dot{p}(\mathbf{x},t\,|\,\mathbf{s},0)\right]\times\delta\tau(\mathbf{g},t\,|\,\mathbf{s},0), \tag{7}$$

where the asterisk * represents temporal convolution and $\Delta\delta\tau$ is the recorded data shifted in time and weighted by the associated traveltime residual E:

$$\delta\tau(\mathbf{g},t\,|\,\mathbf{s},0) = -\frac{1}{E}\,\dot{p}\left(\mathbf{g},t-\Delta\tau^t\,|\,\mathbf{s},0\right)^{obs}\Delta\tau^t(\mathbf{g},t\,|\,\mathbf{s},0). \tag{8}$$

Here the backpropagated residual wavefield g_{bk} in equation (7) is calculated by solving the adjoint visco-acoustic wave equations (Blanch et al., 1995) as

$$\begin{aligned} &\frac{\partial q}{\partial t} + \nabla\cdot\left(\frac{1}{\rho}\mathbf{u}\right) = -\Delta d\left(\mathbf{x}_g,t;\mathbf{x}_S\right), \\ &\frac{\partial \mathbf{u}}{\partial t} + \left[\nabla\kappa(1+\tau)q + \nabla\frac{\kappa\tau r_q}{\tau_\sigma}\right] = 0, \\ &\frac{\partial r_q}{\partial t} - \frac{r_q}{\tau_\sigma} - q = 0, \end{aligned} \tag{9}$$

where q, $\mathbf{u}$ and r_q are respectively the adjoint state variables of the pressure wavefield P, the particle velocity vector $\mathbf{v}$, and the memory variable r_p in equation (5). Assuming only the pressure seismograms are recorded, the residual vector $\Delta\boldsymbol{d}$ will have only one component as $\Delta\boldsymbol{d} = [\Delta d\ 0\ 0]^t$, which is also recognized as the virtual source term. The adjoint equations can help to correct for the phase change in the solution to the visco-acoustic wave equations and to migrate the subsurface structures at the correct depths, making the misfit function converge faster with better gradients. The search direction β is updated using the conjugate gradient method (Nocedal and Wright, 2006).

SENSITIVITY OF THE VELOCITY TO *Q*

In this study, the attenuation varies with frequencies while Q does not. So the constant Q theorem (Kjartansson, 1979) can be used to analyze the velocity and traveltime change with respect to different Q models. For a homogeneous and lossy medium with velocity c_0, a quality factor Q and a monochromatic point source with angular frequency ω, the complex phase velocity of the waves in this medium is

$$c(\omega) = c_0\left[1+\frac{1}{\pi Q}\ln\frac{\omega}{\omega_0}\right]\left(1-\frac{i}{2Q}\right), \tag{10}$$

where i is the imaginary unit. To simplify equation (10) (Kjartansson, 1979), if $Q^{-2} \ll 1$, we have

$$c \approx c_0\,|\frac{\omega}{\omega_0}|^{1/(\pi Q)}. \tag{11}$$

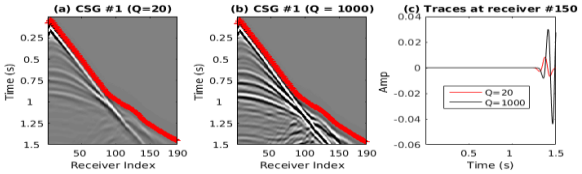

Figure 1: CSGs associated with (a) Q = 20, and (b) 1000 generated from the Marmousi model shown in Figure 2(a). (c) Two traces at the 150th receiver location.

Based on this approximation, the velocity c is slightly dependent on the ratio between the frequency ω and the reference frequency ω_0. It can be estimated that waves of higher frequencies are usually attenuated more than the low frequency parts in the propagation (Gaurav and Schuster, 2014). If Q is greater than 100, the attenuation can nearly be neglected and $c \approx c_0$ holds except for very low or very high frequencies according to equation (11). However, the waves of high frequencies $\omega > \omega_0$ can still be recorded by receivers although some of them are attenuated in propagation at the speed $c > c_0$ through the medium with a small Q. Therefore, these waves can bring the first breaks arrive earlier than in the pure acoustic medium. We setup Q = 20, and 1000 to illustrate this idea in Figures 1(a-c).

NUMERICAL TESTS

Visco-acoustic WT is now applied to synthetic data. The observed data is simulated by solving equation (5) using the staggered grid method (Virieux, 1986) based on a

Marmousi model (Figure 2(a)) with Q = 20. A smoothed version of this true model is presented in Figure 2(b) for further comparison since WT mostly reconstruct the low-intermediate wavenumber parts of the velocity model.

In the inversion test 1, the initial model is a very smoothed version (Figure 3(a)) of the true Marmousi model. The model size is 1098 *m* in the vertical Z direction and 3450 *m* in the horizontal X direction with a grid spacing of 6 *m*. The data are recorded by 190 receivers spaced at an interval of 18 *m*, and are triggered by 60 sources with a spacing of 54 *m*. The source wavelet is a Ricker wavelet with a peak frequency of 10 Hz. The velocity is inverted by the proposed WT method in the methodology section with Q = 20, 50, and 1000. The tomograms after 15 iterations are shown in Figures 3(b-d). In this test, we notice that the inverted tomogram based on a correct Q value is more consistent with the true velocity model while the other inverted tomograms are not too far away from the true model. Improvements for areas at X = 1800 *m* and Z = 720 *m* can be clearly discerned in Figures 3(b) and (c) compared to Figure 3(d). The data comparisons along with the model misfits are also shown in Figures 4(a-e). In Figure 4(e), all the first breaks of the four traces are almost aligned at the same moment, which implies that a good initial velocity model can converge to a good WT inversion result regardless of the background Q. To verify if all of the inversions with different Q's approximate the true model, we then use the WT inverted tomograms (Figures 3(b-d)) as the starting velocity models for FWI, and the results are presented in Figures 5(a-c). Therefore, by comparison, a good estimation of the Q model is beneficial to the final FWI tomograms for both the shallow and deep parts.

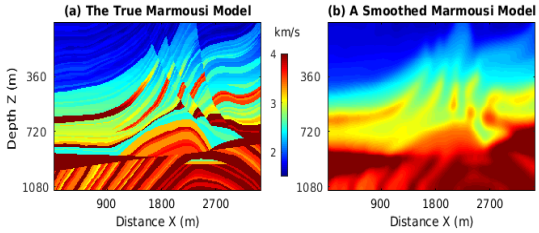

Figure 2: (a) The true Marmousi velocity model, and (b) its smoothed version for computing model residuals.

In test 2, a different 1D model (Figure 6(a)) is used as a starting model for the inversion based on the same data set and acquisition geometry. The inverted tomograms are presented in Figures 6(b-d) with the three different Q values. With an unideal or sometimes faulty initial model, the WT method still recovers some subspace structures of low-intermediate wavenumbers from the visco-acoustic data with Q = 20 and 50. However, if the attenuation is almost neglected by assigning Q = 1000, the inversion cannot converge any more, as shown in Figure 6(d). It implies that the velocity cannot be updated in this situation because its sensitivity to the Q model, which is far from the true one, should not be ignored. The diverged blue line in Figure 7(e) also shows an imperfect starting velocity model can be very sensitive to the attenuation in the inversion.

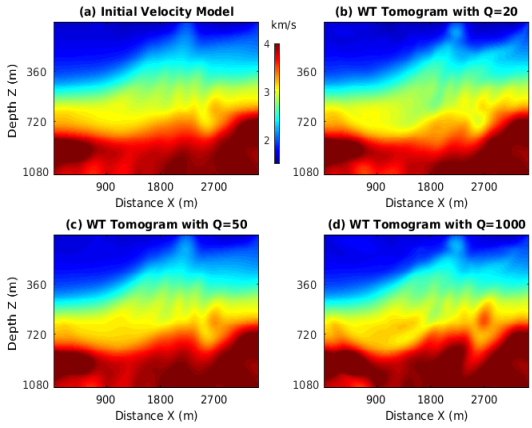

Figure 3: (a) The starting velocity model for WT, the WT inverted tomograms with Q = (b) 20, (c) 50, and (d) 1000.

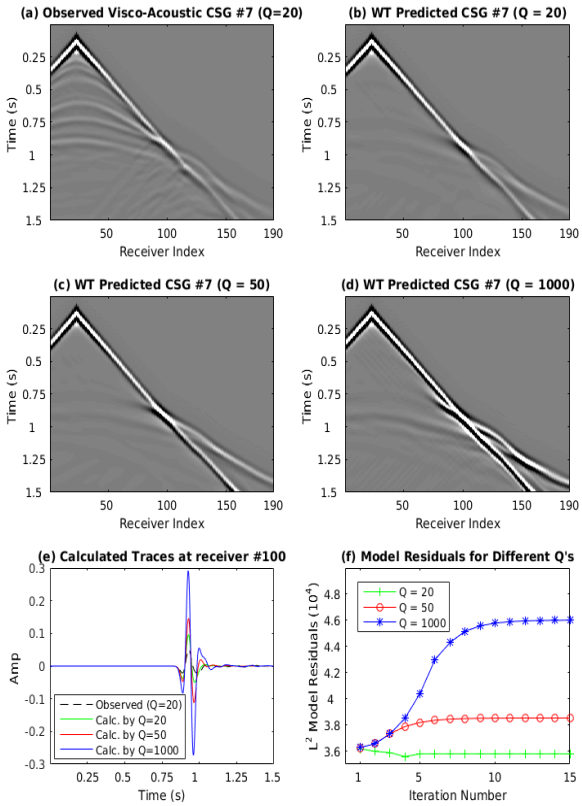

Figure 4: (a) The observed CSG #7, and the CSGs #7 calculated after 15 iterations by WT with Q = (b) 20, (c) 50,

and (d) 1000. (e) A comparison between the observed and the predicted traces at receiver #100. (f) The model residuals of the inverted tomograms compared to Figure 1(b).

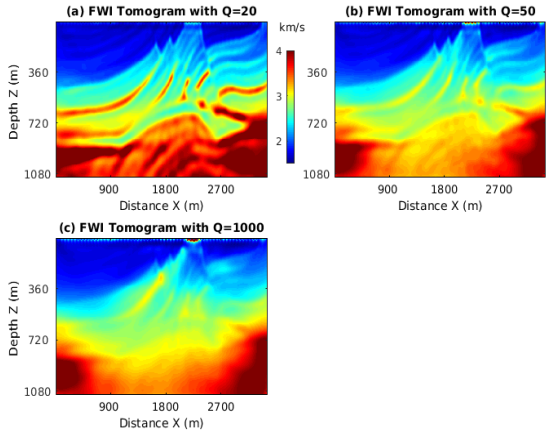

Figure 5: FWI tomograms (a-c) with Q = 20, 50, and 1000, using different starting models in Figures 2(b-d), respectively.

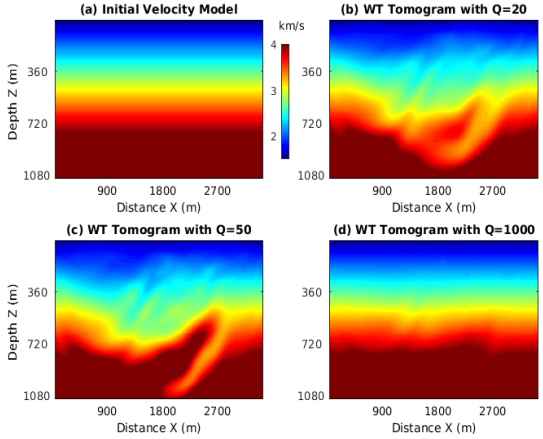

Figure 6: (a) The 1d initial velocity model for WT, the WT inverted tomograms with Q = (b) 20, (c) 50, and (d) 1000.

CONCLUSIONS

A visco-acoustic wave equation traveltime inversion can be used to invert for a better background velocity model with correct attenuation profiles. In order to clarify the sensitivity of the velocity variations to Q, we carry out the numerical tests with three different homogeneous Q models for comparisons, although the background Q model is usually set according to rock physics or from the inversion results. If the initial background velocity model is consistent with the true model, a reasonable WT tomogram can be possibly expected regardless of Q models. If the starting velocity model is not ideal, a relatively accurate estimation of the background Q value is important for updating the velocity distribution because an incorrect Q distribution can mislead the inversion from the beginning. Our future work is to carry out the hybrid inversion of the attenuation and the velocity distributions together.

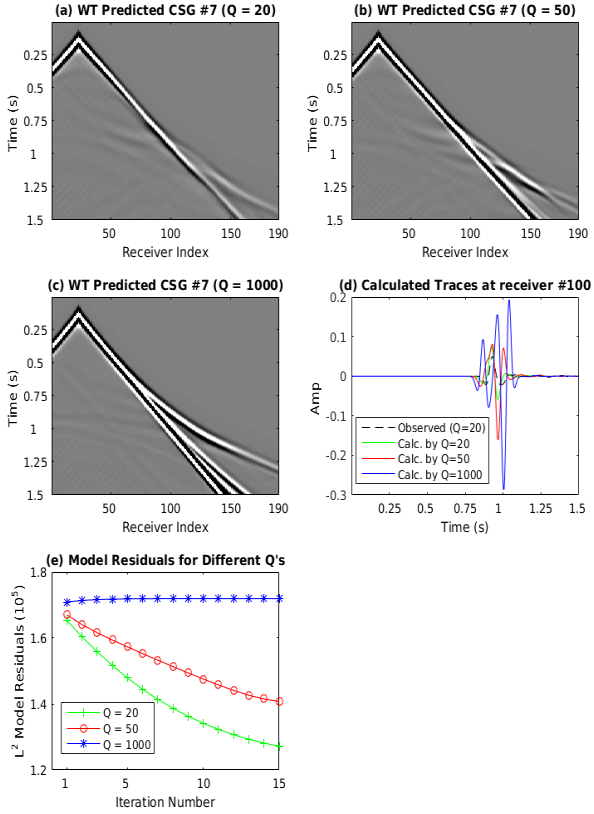

Figure 7: The CSGs #7 (a-c) calculated after 15 iterations by WT with tomograms in Figures 6(b-d) and with Q = 20, 50, and 1000, respectively, (d) a comparison between the observed and the predicted traces at receiver #100, and (e) the model residuals of the inverted tomograms compared to Figure 2(b).

ACKNOWLEDGMENTS

We thank the King Abdullah University of Science and Technology (KAUST) and the sponsors of the CSIM consortium for their support. We are also grateful to the high performance computing center (HPC) of KAUST for prividing access to the supercomputing facilities. We would also appreciate the support of National Natural Science Foundation of China (grants 11501302 and 61571238), and the Scientific and Technological Support Project (Society) of Jiangsu Province (grant BE2016776).

EDITED REFERENCES

Note: This reference list is a copyedited version of the reference list submitted by the author. Reference lists for the 2017 SEG Technical Program Expanded Abstracts have been copyedited so that references provided with the online metadata for each paper will achieve a high degree of linking to cited sources that appear on the Web.

REFERENCES

Aki, K., and P. G. Richards, 2002, Quantitative seismology, 1.

Blanch, J. O., J. O. A. Robertsson, and W. W. Symes, 1995, Modeling of a constant Q: Methodology and algorithm for an efficient and optimally inexpensive viscoelastic technique: Geophysics, **60**, 176–184, http://dx.doi.org/10.1190/1.1443744

Dutta, G., and G. T. Schuster, 2014, Attenuation compensation for least-squares reverse time migration using the visco-acoustic wave equation: Geophysics, **79**, no. 6, S251–S262, http://dx.doi.org/10.1190/geo2013-0414.1.

Feng, S., and G. Schuster, 2016, Anisotropic wave-equation traveltime and waveform inversion: 86th Annual International Meeting, SEG, Expanded Abstracts, 1196–1200, http://dx.doi.org/10.1190/segam2016-13818024.1.

Kjartansson, E., 1979, Constant *Q*-wave propagation and attenuation: Journal of Geophysical Research: Solid Earth, **84**, 4737–4748, http://dx.doi.org/10.1029/JB084iB09p04737.

Luo, Y., and G. T. Schuster, 1991a, Wave equation inversion of skeletalized geophysical data: Geophysical Journal International, **105**, 289–294, http://dx.doi.org/10.1111/gji.1991.105.issue-2.

Luo, Y., and G. T. Schuster, 1991b, Wave-equation traveltime inversion: Geophysics, **56**, 645–653, http://dx.doi.org/10.1190/1.1443081.

Nocedal, J., and S. J. Wright, 2006, Sequential quadratic programming: Springer, http://dx.doi.org/10.1007/978-0-387-40065-5_18.

Robertson, S. E., and S. Walker, 1994, Some simple effective approximations to the 2-Poisson model for probabilistic weighted retrieval: Proceedings of the 17th Annual International ACM SIGIR Conference on Research and Development in Information Retrieval, Springer-Verlag, 232–241, https://doi.org/10.1007/978-1-4471-2099-5_24.

Tarantola, A., 2005, Inverse problem theory and methods for model parameter estimation: SIAM, https://doi.org/10.1137/1.9780898717921.

Virieux, J., 1986, P-SV wave propagation in heterogeneous media: Velocity-stress finite-difference method: Geophysics, **51**, 889–901, http://dx.doi.org/10.1190/1.1442147.

Virieux, J., and S. Operto, 2009, An overview of full-waveform inversion in exploration geophysics: Geophysics, **74**, no. 6, WCC1–WCC26, http://dx.doi.org/10.1190/1.3238367.